

Investigation into Coatings Produced from
Nanoparticle Blended Feedstock for Rotating
Equipment Repair Applications

Albara B. Al-Askandarani

MEng

2011

**Investigation into Coatings Produced from Nanoparticle Blended
Feedstock for Rotating Equipment Repair Applications**

By

Albara Basim Al-Askandarani

BSc in Mechanical Engineering (USF) USA, 2007

This thesis is submitted to Dublin City University as the fulfillment of the
requirement for award of degree of

Master of Engineering (MEng)

Research Supervisors

Professor M.S.J. Hashmi (D.Sc, Ph.D, CEng., FIMechE., FIEI, MASME)

Professor B.S. Yilbas (D.Eng., Ph.D, MASME)

**School of Mechanical & Manufacturing Engineering
Dublin City University**

May 2011

DECLARATION

I hereby certify that this material, which I now submit for assessment on the programme of study leading to the award of Master's of Engineering (MEng) is entirely my own work, that I have exercised reasonable care to ensure that the work is original, and does not to the best of my knowledge breach any law of copyright, and has not been taken from the work of others save and to the extent that such work has been cited and acknowledged within the text of my work.

Signed: _____

ID No. 57127361

Date: _____

ACKNOWLEDGEMENTS

I would like to express my gratitude to my supervisors, **Professor M.S.J. Hashmi** and **Professor B.S. Yilbas** for their guidance and support during my study.

Also, I am sincerely grateful to my mother, father, brothers and sisters for their support, prayers and patience. Working and studying simultaneously was not an easy task, but my mother's encouragement and desire for my development have indeed motivated me to complete this work.

This work would not have been possible without the mentorship of **Dr. Hussain Al-Fadhli**, who committed himself and dedicated much of his personal time and effort as means of support.

I am heartfully thankful to my colleagues that assisted me in this work including **Omer Osman, Dr. Ihsan Taie, Meshary Ghannam, Marwan Khazendar** and **Saad Ali**.

Lastly, the support of the management of the Mechanical Services Shops Department of Saudi Aramco is praise worthy as it was the major contributor to the success of this work.

Title of Thesis: Investigation into Coatings Produced from Nano Particle Blended Feedstock for Rotating Equipment Repair Applications

Name of Student: Albara B. Al-Askandarani **Student Number:** 57127361

ABSTRACT

Coating of carbon steel with conventional and nano particle blended feedstock material is considered in relation to repair applications of rotating equipment. Gas Metal Arc Welding (GMAW) and Wire Arc Spray (WAS) processes are used to produce the coatings on carbon steel workpieces. The wire arc sprayed workpieces are heat treated at temperature similar to the operating temperature of hot-path components of power gas turbines. The microstructure and metallurgy of the workpieces are examined using the Scanning Electron Microscope (SEM), Optical Microscope, Energy Dispersive Spectroscopy (EDS), X-ray Diffraction (XRD). The indentation tests are carried out to assess the microhardness variation across the coatings. In the case of coatings produced by GMAW, it is found that fine structures are formed in the coating due to the presence of nano particles and they resulted in increased microhardness of the coatings. In the case of the wire arc sprayed workpieces, the formation of dimples like structure at the surface increases the surface roughness of the coatings. In addition, the microhardness of the resulting coating is significantly higher than that of the base material. The heat treatment does not alter the microstructure and microhardness of the coatings significantly.

Table of Contents

	<i>Page</i>
Declaration	I
Acknowledgements	II
Abstract	III
Table of Contents	IV
List of Tables	VII
List of Figures	VIII
Chapter 1 – Introduction	1
1.1 Nano Technology in Relation to Repair Applications.....	1
1.2 Thermal Spray Technology.....	4
1.3 Welding Overlay Coating.....	7
1.4 Maintenance of Rotating Equipment and its Importance.....	9
1.5 Testing and Development of Coatings Related to Rotating Equipment Repair.....	12
1.6 Project Objectives and Thesis Outline.....	12
Chapter 2 – Literature Review	15
2.0 Introduction.....	15
2.1 Characterization and Mechanical Properties of Nano Structured Coatings.....	15
2.2 Wear and Tribological Properties of Nano Structured Coatings.....	20

2.3 Effects of Heat Treatment on Nano Structured Coating.....	24
2.4 Comparison Between Properties of Microstructured and Nano Structured Coatings.....	28
2.5 Effects of Coating Process Parameters of Nano Structured Coatings...	31
2.6 Summary of Literature Review.....	35
Chapter 3 – Experimental Equipment & Procedures.....	37
3.0 Introduction.....	37
3.1 Specimen Design.....	37
3.2 Gas Metal Arc Welding.....	38
3.2.1 Gas Metal Arc Welding Feedstock.....	38
3.2.1.1 Conventional GMAW Feedstock.....	38
3.2.1.2 Nano Structured GMAW Feedstock.....	39
3.2.2 Gas Metal Arc Welding Process.....	40
3.3 Wire Arc Spray.....	41
3.3.1 Wire Arc Spray Consumables.....	41
3.3.1.1 Conventional Wire Arc Spray feedstock.....	41
3.3.1.2 Nano Structured Wire Arc Spray Consumables.....	42
3.3.2 Wire Arc Spray Process.....	42
3.4 SEM, EDS and Optical Microscope.....	43
3.5 X-ray Diffraction (XRD).....	44
3.6 Indentation Tests.....	46
3.7 Heat Treatment.....	47

Chapter 4 – Results and Discussions	48
4.1 Coating Produced By Deposition of Nano Particles Blended Wires....	48
4.2 Wire Arc Sprayed Nano structured Coatings.....	55
5.0 Conclusions and suggestions for future work	65
5.1 Coating Produced by Deposition of Nano Particles Blended Wire.....	65
5.2 Wire Arc Sprayed Nano Structured Coatings.....	66
Suggestions for Future Work	68
References	70
Publications by the author	75

List of Tables

		<i>Page</i>
3.1	Chemical composition of conventional wire material [wt.-%].....	38
3.2	Chemical composition of nano structured wire material [wt.-%].....	39
3.3	Welding parameters.....	40
3.4	Chemical composition of conventional wire material [wt.-%].....	41
3.5	Chemical composition of nano structured wire material [wt.-%].....	42
3.6	Wire arc spray parameters.....	43
3.7	XRD machine Specifications.....	45
4.1	Microhardness of the coating and the base material.....	55
4.2	EDS results across the cross-section of the workpiece and SEM micrograph for the cross-section showing EDS spectrums.....	63
4.3	Microhardness results for the base material, arc sprayed prior and after the heat treatment process.....	64

List of Figures

		<u>Page</u>
1.1	Schematic of Wire Arc Spray System.....	6
1.2	Gas Metal Arc Welding System.....	9
1.3	Cross-section of a combustion gas turbine.....	11
3.1	Scanning Electron Microscope model JEOL JDX 3530 LV.....	44
3.2	X-ray Diffraction model Beuker D8 Advance.....	45
3.3	Indentation Hardness Tester manufactured by BUEHLER Com.....	46
4.1	Optical micrographs of coating surface and cross-section.....	49
4.2	EDS line scan for elemental composition of coating.....	50
4.3	SEM and optical micrographs of conventional and nano structured coating cross-sections.....	52
4.4	SEM micrographs of cross-sectional views of nano structured coating.....	54
4.5	Optical micrograph of cross-sectional view of nano structured coating and indentation marks.....	55
4.6	SEM micrographs of top surface of arc sprayed coating prior and after the heat treatment process.....	57
4.7	Surface roughness of the arc sprayed coating.....	58
4.8	XRD Diffratogram for coating prior and after heat treatment.....	59
4.9	SEM micrographs of cross-section of the workpieces prior and after heat treatment.....	61
4.10	SEM micrograph for the cross-section showing EDS spectrums.....	63
4.11	Indentation marks on the cross-section of the workpiece.....	65

Chapter 1 – Introduction

With the worlds' increasing demand for energy, utilizing advanced technologies that enable increased operational and maintenance efficiency at various energy producing and processing facilities becomes essential. Rotating equipment, for instance, is a fertile area to utilize latest technologies especially during the repair stage. Advanced surface treatments and coatings enable the repair of rotating equipment's critical parts at a reduced cost. Not only that, but also minimizing failure reoccurrence, enabling operation under more severe conditions and enhancing the efficiency are examples of the benefits of utilizing such technologies.

1.1 Nano Technology in Relation to Repair Applications

In recent years, nano technology gained popularity amongst scientists, researchers and manufacturers due to the extraordinary results that can be achieved by controlling the material structure at the nano (atomic) scale. The term nano technology was first introduced to literature by Professor Norio Taniguchi of Tokyo Science University in 1974, who defined it as: "Nano technology' mainly consists of the processing of, separation,

consolidation, and deformation of materials by one atom or by one molecule." [1]. Ever since, scientists and researchers were able to achieve materials of unique properties. Combined with the new highly advanced microscopic and fabrication devices that can precisely view and control matter at an atomic scale, nano technology has been rapidly developing.

The desired nano materials are produced by bottom-up, and top-down approaches. In the bottom-up approaches, nano scale components are arranged to form complex assemblies. These approaches are achievable by utilizing various methods including molecular self-assembly and chemical synthesis. On the other hand, in the top-down approaches, larger devices are used to direct the assembly of smaller devices. The processes used in the top-down approaches include atomic force microscope, nanolithography and focused ion beams.

Since nano technology is used as a tool to complement, develop and advance different applications, surface treatments and coatings have greatly benefited from this technology. A coating is a relatively thin layer of material that is applied to cover a substrate. Coatings are utilized for a variety of reasons. One of the most common industrial needs for coatings is to improve the surface properties of a substrate. The improved properties include wear resistance, corrosion resistance and thermal

conductivity/insulation [2]. Furthermore, cost saving by applying advanced surface treatments and coatings during design and repair stages of rotating equipment, for instance, has been proven valid. For example, the use of expensive high strength materials and super alloys can be mitigated or omitted by using low grade materials that are coated with a layer of material, which is compatible with the media and service. Depending upon the coating process, coating material and desired function, the coating properties differ. In the majority of applications, the most important coating process properties include thickness, porosity, adhesion, deposition rate and surface finish. Based on the desired coating properties, the optimum coating process may be selected.

One way of combining the emerging technologies with the existing rotating equipment repair processes is the use of nanotechnology developed materials in thermal spray and weld overlay in rotating equipment repair. Both processes have been extensively used for the refurbishment of rotating equipment components for decades. Each refurbishment process has its advantages and disadvantages and is selected based on the specific application and required properties.

1.2 Thermal Spray Technology

Several thermal spray processes have been in existence since the early 1900's. Some processes are capable of producing coatings from a large variety of materials and are able to produce coatings with optimum properties, but are costly to acquire and apply. On the other hand, other thermal spray processes have limitations, but are affordable to acquire and apply. Wire arc spray, for example, is one form of thermal spray that is commonly used in rotating equipment repair facilities due to its affordability and desirable produced coating properties. Generally, thermal spray processes are divided into two main categories, based on the source of heat that melts the coating material: Combustion and arc spray.

In combustion thermal spray processes, fuel combustion is used to provide temperatures that are elevated enough to melt the coating feedstock material. The most common types of fuel used in these processes are propane, kerosene and acetylene. The proper combustion air/fuel ratio can be achieved by setting the proper air or oxygen flow and pressure as well as the fuel flow and pressure. By using the combustion as a heat source, it is possible to produce coatings from a variety of materials including polymers and metals. The coating material could be

either in the wire or powder form. High Velocity Oxy-Fuel, flame spray and metalizing are common thermal spray processes that use combustion as a heat source.

Arc spray, on the other hand, works by a different principle. Instead of combusting fuel, electric discharge arc is used to directly or indirectly melt the coating material. For example, in plasma arc spray, an electric arc is used to indirectly melt the coating material by creating a plasma flame. The plasma flame is achieved by ionizing an inert gas such as argon, nitrogen, helium or hydrogen. The inert gas temperature must be increased to elevated levels, to reach the ionization state of the gas. As a result, an electric arc, which has a temperature in excess of 5,000 K, is used and maintained along with the constant flow of the inert gas to maintain the plasma flame. Using plasma as a heat source, it is possible to thermally spray a wide range of materials that is not limited to polymers and metals only, but also extended to high melting temperature materials such as ceramics. The coating material is generally in the powder form.

Another example of arc spray coating is wire arc spray, which is examined in this study. Electric discharge arc is used to directly melt the coating material. As illustrated in Figure 1.1 [3], the coating process consists of two consumable coating wires of identical or different

materials that are continuously fed into a gun. With one of the wires having a positive electric polarity and the other having a negative electric polarity, an electric arc is formed between the two wires to complete the electric circuit. The electric arc rapidly raises the temperature of both wires and melts them. The molten material is then projected onto the substrate by compressed air or gas. The coating wire material is limited to electrically conductive materials. However, it is possible to add non-electrically conductive materials, such as carbides, in the core of hollow metallic wires to achieve the desired properties. In this work, for instance, hollow wires that are filled with carbides and nano particles were examined. Some of the main advantages of using wire arc spray include cost effectiveness, fast deposition rates, and minimal heat transfer to the substrate.

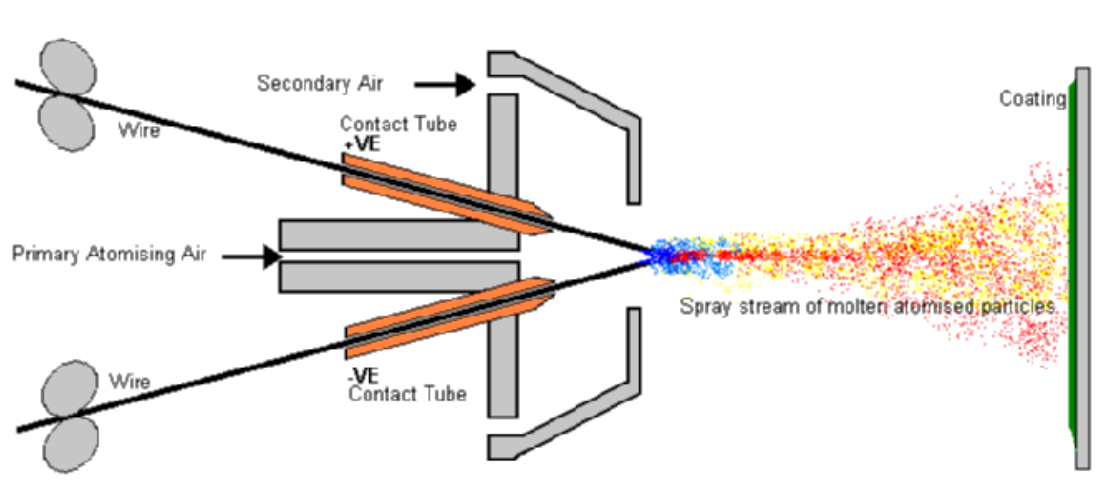


Figure 1.1. Schematic of Wire Arc Spray System [3].

1.3 Welding Overlay Coating

Similar to thermal spray, metal overlay coatings can be achieved by a variety of welding processes. Each welding process has its advantages and disadvantages regarding the deposited material and the effects on the substrate material. Welding is the process of joining workpieces together by localized fusion. This is achievable by heating the fusion area to melting temperatures [4]. Pressure and filler material may or may not be used. On the other hand, coatings produced by welding processes are achieved by fusing filler material with the top surface material of the workpiece.

Analogous to the thermal spray classifications, welding processes are classified by the energy or heat source. Some welding processes date back to ancient times and other processes are newly developed. For example, forge welding is an ancient welding process. The reason behind its existence since centuries ago is the fact that the heat required to forge weld is typically 50 to 90 percent of the workpiece melting temperature. The rest of the energy required to forge weld is gained from the forging or hammering process. On the contrary, laser welding is a welding process that emerged during recent years and it is a process that is still developing. The term "LASER" stands for Light Amplification by

Stimulated Emission of Radiation [5]. Several laser sources exist and are selected based on the application. Furthermore, precise control of the laser properties could be finely adjusted to weld, or produce coatings of desired properties. An example of coating using the laser welding process is laser metal deposition.

From the ancient to the most sophisticated welding processes, the majority of the processes are still in existence today. Some material properties can only be achieved by the primitive welding process, while other applications require state of the art emerging welding technologies. For example, in industrial manufacturing and refurbishment, an efficient, easy to use and reliable high deposition rate welding process is generally preferred. As such, gas metal arc welding is a welding process that matches most of the industrial needs. The welding process takes place by one of several metal transfer modes. The main metal transfer modes are short circuiting, globular mode and spray. GMAW equipment consists of a power supply, electrode wire feed unit, electrode wire and shielding gas (Figure 1.2) [6]. The power settings can be adjusted based on the substrate material type and thickness as well as the desired metal transfer mode. Furthermore, the electrode wire material selection, when considering weld overlay and coating by GMAW, is very critical to

achieve the required properties. Also, advanced research and development in that area is essential. Another advantage of GMAW is the fact that the settings could be adjusted to increase the productivity and production rates, or to achieve higher quality welds and coatings with minimized heat affected zones, weld dilution, and minimized distortion to the workpiece.

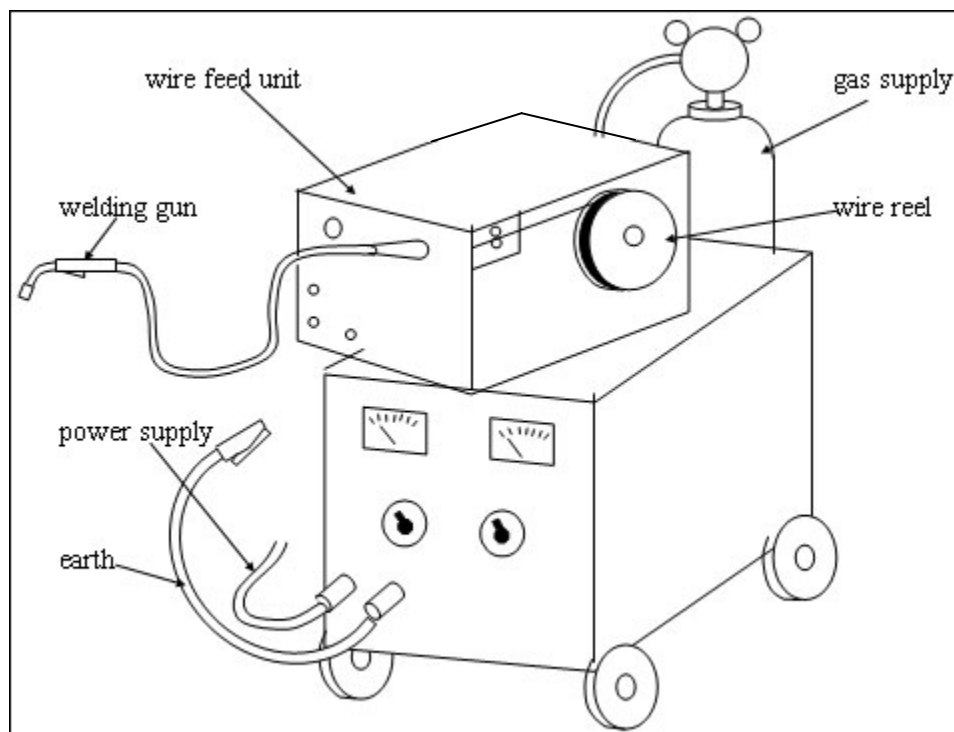


Figure 1.2. Gas Metal Arc Welding System [6].

1.4 Maintenance of Rotating Equipment and its Importance

Rotating equipment in the energy industry, such as gas turbines, steam turbines, compressors, pumps and electric motors often operate under severe environments. The materials within rotating equipment are often

subjected to elevated temperatures, high erosion rates, cyclic loadings, wear and other material deteriorating conditions. As such, research and development and application of newly emerging and advanced technologies in the field of surface treatment have enabled increasing the efficiency, reliability and productivity of such machinery.

For example, the efficiency of gas turbines (Figure 1.3) [7] is directly related to the combustion process. Theoretically, a stoichiometric fuel/air ratio yields optimum combustion efficiency, since all fuel molecules are combusted. Not only enhanced efficiency is achieved by stoichiometric fuel/air ratio, but also toxic emissions are minimized, which is favorable for the environment. Other advantages include increased temperature, which can be utilized in cogeneration and heat recovery cycles, in an effort to enhance the thermodynamic efficiency. On the other hand, increased temperatures will also result in rapid deterioration of the materials that are directly exposed to combustion including combustion baskets, transition pieces and turbine inlet vanes.

The combustion components of gas turbines are often inspected in intervals, based on the size of gas turbine, material quality and operational performance. During each combustion inspection, the gas turbine must be put out of service to conduct the inspection and testing to

ensure the integrity of the components. As a result, there is production loss associated with carrying the combustion inspection. Furthermore, the disassembly, inspection, testing, repair and re-assembly add to the overall maintenance costs. As a result, increasing the intervals between the inspections saves cost on the longer run and is desirable.

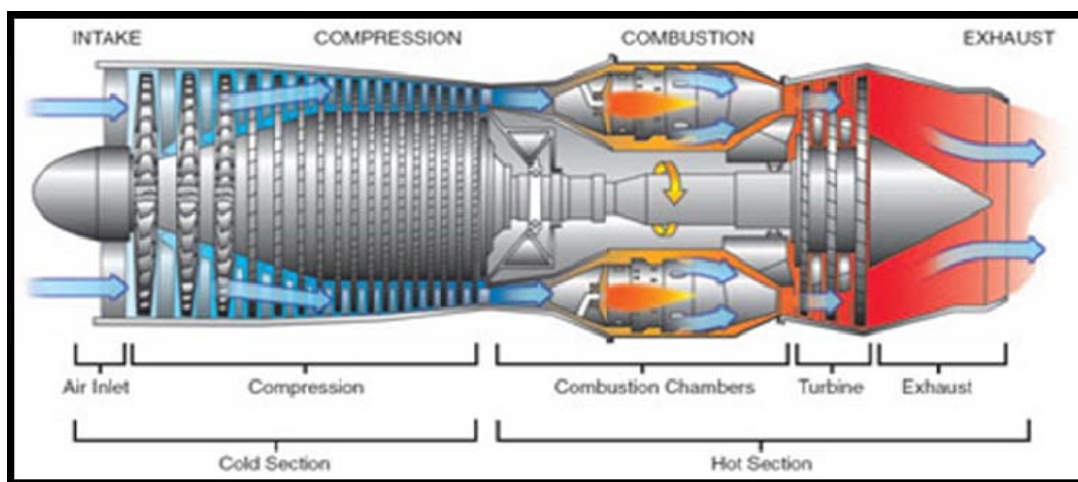


Figure 1.3. Cross-section of a combustion gas turbine [7].

One of the methods that can be utilized to allow operating gas turbines at higher combustion temperatures as well as increasing the intervals between inspections is the use of advanced coatings and surface treatments. Various gas turbine manufacturers offer standard combustion parts and enhanced life combustion parts, which are coated with manufacturer patented materials. Also, the enhanced life parts often cost more than the double of the cost regular parts.

1.5 Testing and Development of Coatings Related to Rotating Equipment Repair

To be able to properly assess the performance of coatings onto substrates, it is important to test, inspect and measure the properties of coating. Depending on the intended use of the coating, the proper testing and properties measurements vary. In this particular work, the examined coating is intended to be used in hot path parts of gas turbines, which undergo high temperatures. Consequently, the main material deterioration factor is the high temperature. This could be simulated by heat treating the coated workpieces to similar temperatures and closely examining the morphology and micrography of the coated material.

Coating of metallic surfaces via welding deposition and wire arc spray finds wide applications in parts repair. This is because of the practicality, low cost and the capability of achieving improved metallurgical and mechanical properties. However, the coating material is expected to be similar or identical to the base material to avoid the mismatch in terms of metallurgical and mechanical properties.

1.6 Project Objectives and Thesis Outline

The development of nanotechnology enables to reinforce and/or improve the metallurgical and mechanical properties of the deposited layer.

Moreover, depending upon the nano particles blended in the wire material and processing parameters, the properties of the resulting coating change. In this work, coating of carbon steel using the nano structured wire material is carried out and metallurgical and morphological changes in the resulting coating are examined. The coating is produced by different processes, which are the gas metal arc welding and the wire arc spray. Both coatings, by gas metal arc welding and arc spray, are produced using the wire material, which is blended with nano particles. By adding nano particles, the properties of the deposited material are expected to be enhanced. Consequently, investigation of the resulting coating properties becomes essential. The objective of the present study is to investigate the metallurgical and morphological changes in the coatings produced by arc spraying and gas metal arc welding processes using the conventional and nano structured wires.

The thesis consists of five chapters. The first chapter introduces nanotechnology, thermal spray, welding and the importance of maintenance of gas turbines. The second chapter is a literature survey that summarizes the findings and conclusions of other literature with regards to application of coatings and materials that contain nano particles. The survey covered several different topics regarding nano structured coatings

including Characterization and mechanical properties, wear and tribological properties, effects of heat treatment, comparison between properties of microstructured and nano structured coatings and the effects of coating process parameters. Chapter three of the thesis is about the equipment used for the experiment. Furthermore, it discusses the workpiece preparation, weld deposition and thermal spray process parameters, procedures and considerations pertaining to the experiment. The morphological and metallurgical tests using microscopy, EDS, SEM and XRD will be elaborated as well. In addition, hardness testing using Vickers indentation test of thermally sprayed workpiece will also included in this chapter. In chapter four, results of the experimental work are discussed. Furthermore, the effect of heat treatment and comparison between conventional coatings and coatings containing nano particles are included in the chapter. Finally, chapter five presents the conclusions and suggested future work related to the subject.

Chapter 2 – Literature Review

2.0 Introduction

The following presents the studies reported in the open literature with regards to properties and metallurgical characteristics of nano structured coatings. Furthermore, the influences of the coating process parameters and heat treatment on the properties of the coatings produced are included. Other studies in the open literature compared the microstructured and nano structured coatings and evaluated them accordingly.

The latest up to date published work and advancements are included in the literature survey, which are categorized under the relevant sub-headings.

2.1 Characterization and Mechanical Properties of Nano Structured Coatings

The characteristics of nano particles and their effects on the formation of structures in air plasma spraying of WC-17Co coating were investigated by Chen et al. [8]. Nano structured coating was developed during the plasma spraying process while using the 2-5 nm size coating sub-particles. Acting as crystallization nuclei, the sub-particles resulted in

finer grains during the plasma spray process, which was desirable to form nano structures in the coating. The original coating material contained particles in the size ranging 50-500 nm and sub-particles in the size range of 2-5 nm. The nano structured coating resulted in improved micro-hardness, fracture toughness and bonding strength.

Thermal spray feedstock characteristics directly influenced the resulting coatings. Kim et al. [9] studied the influence of the feedstock characteristics on the resulting HVOF WC-Co coatings. By examining the morphology of the existing nano structured WC-Co commercial feedstock for HVOF coating, it was found that the feedstock powders had irregular shapes with a large amount of pores. The excessive melting of different particles took place because of the large surface to volume ratio. By developing densely packed spherical shaped nano structured feedstock powders with low porosity, the resulted coating had improved properties, including density, microhardness and wear resistance.

Zhu et al. [10] examined the deposition characterization of nano structured WC-Co coatings. It was found that the produced coatings mainly consisted of structures that contained WC grains similar to that of the primary powder, with mean particle size of 35 nm. On the other hand, different particle sizes were found, as a result of the non-uniform

temperature distribution within the plasma flame. Furthermore, the temperature in the center of the plasma flame was higher, 15000 °C, when compared with temperature towards the edges, 1000 °C. In addition, WC grains with 10 nm size were formed as a result of melting. Other regions consisted of completely amorphous phase because of complete melting of the WC-Co powders. Also, grain growth of some WC grains to 100 nm was observed in addition to the grains that went through recrystallization, which resulted in strip and square shaped structures with sizes up to 500 nm.

The microstructural characteristics of cold-sprayed nano structured WC-Co coatings were examined by Lima et al. [11]. SEM and microscopy of the coating cross-section revealed that dense and low porosity coatings were produced without cracks. In addition, since cold-spray is a solid state process, the coating was produced by densification of the feedstock powder upon supersonic velocity impact of the particles, rather than melting. The densification was also confirmed by comparing the microhardness of the feedstock powder and produced coatings, which have increased 30 times during the coating process. Phase composition of the coating via XRD revealed that only a crystalline phase WC and some Co were present. However, no other phases were present, which

confirmed that no degradation of the particles took place. Also, compressive residual stresses were developed during the coating process, not because of high temperature, but because of a shot-peening effect as a result of the particles impact against the substrate at supersonic velocities.

Interfacial mechanical properties of plasma-sprayed Al₂O₃-13wt%TiO₂ nanocrystalline and conventional coatings were examined by Bansal et al. [12]. They used rockwell indentation method to assess the interfacial toughness. It was found that the nanocrystalline coating was superior to the conventional coating. Microstructural examination of the interface between the substrate and coating revealed that the conventional coating consisted of fully molten splats. On the other hand, the nanocrystalline coating exhibited a bimodal microstructure consisting of fully molten splats as well as partially molten splats. The fully molten interface of both the conventional and nanocrytalline coating had cracks prior to mechanical testing. On the other hand, a crack free interface with better adhesion was observed in the partially molten splats interface in the nanocrystalline coating due to the presence of TiO₂-rich amorphous phase.

Zeng et al. [13] compared the mechanical properties and metallurgical characteristics of different sizes of nano structured alumina plasma

sprayed coatings. Three feedstock powders were incorporated A, T and F with F powder having the smallest grain size. XRD analysis of the feedstock powders pre and post plasma spray indicated that change in phase composition took place as a result of the coating process. Furthermore, SEM images revealed that the coatings produced by A and T coatings consisted of porous splats that were poorly adhered to each others. On the other hand, the F coating was dense, smooth and consisted of a polished-like surface structure. Also, the F coating, which had the smallest grain size, resulted in improved mechanical properties. The microhardness of F coating was considerably high and the surface roughness average was significantly low in comparison with coatings A and T.

Kim et al. [14] examined the properties of superhard nano WC-12%Co coating by cold spray deposition. It was found that the cold spray deposition process prevented the degradation and decomposition of WC as opposed to other coating processes such as high velocity oxy-fuel. Furthermore, the nano sized WC particles in the feedstock powder maintained the same size after being deposited. Also, the produced coatings had low porosity and very high hardness value of 2050 HV.

2.2 Wear and Tribological Properties of Nano Structured Coatings

Comparison between the wear properties of nano and microcrystalline TiC-Ni-based thermal spray coatings using the vacuum plasma spray (VPS) and high velocity oxy-fuel (HVOF) was carried out by Qi et al. [15]. HVOF coatings exhibited lower wear resistance than VPS coating, when the same feedstock nano and microcrystalline powder was used. This was vastly due to the weakening of cohesion among the splats as a result of the oxide species in the HVOF coatings. Furthermore, the nanocrystalline HVOF coatings showed lower wear resistance than the microcrystalline HVOF coatings because of the increased concentration in the oxide zones. On the other hand, nanocrystalline VPS coatings under tough wear conditions had superior wear resistance in comparison with microcrystalline VPS coatings. Also, nanocrystalline VPS coatings kept smooth worn surfaces in comparison with microcrystalline VPS coatings, which was desirable in different applications for maintaining clearances between parts that were required in the industry.

The wear and friction properties of Vacuum Plasma Sprayed nano structured and conventional WC-Co coatings against alumina under dry friction conditions were investigated by Zhu et al. [16]. Under the same load conditions, the nano structured coating exhibited improved

tribological properties in comparison with conventional coating including lower friction and higher wear resistance. The improvement in the nano structured coating was attributed to the increased hardness and fracture toughness. Also, the nano structured coatings resulted in fine WC grains in comparison with the conventional coatings, which resulted in larger WC grains. The finer WC grains did not directly improve the wear resistance; rather this was attributed to the overall increased hardness of the material.

Wear behavior of high velocity suspension flame sprayed Al_2O_3 produced using micron- and nano sized powder suspensions were examined by Bolelli et al. [17]. Using the micron-sized powder, the produced coatings had significantly higher density and hardness as well as lower roughness in comparison with the coatings that were produced using the nano sized powders. The superiority of the coating produced using the micron-sized powder was because of the well-flattened lamellae of similar size that were homogeneously distributed. On the other hand, the coating produced using the nano sized powders had significantly higher porosity and poor mechanical properties.

Roy et al. [18] comparatively evaluated the friction behavior at ambient temperatures of thermally sprayed $\text{Cr}_3\text{C}_2\text{-25(Ni}_{20}\text{Cr)}$ coatings of

conventional and nano crystalline grains. The coefficient of friction of the nano crystalline coating was 20-30% lower than that of the conventional coating. The reduction in the coefficient of friction in the nanocrystalline coating was mainly attributed to the fact that it had 40% lower surface roughness and 20% higher hardness. Additionally, the material loss of the nanocrystalline coating during wear testing occurred by delamination. On the other hand, the material loss in the conventional coating occurred by breaking-out of the particles as a result of the soft matrix.

Chen et al. [19] examined the tribological properties of nano structured zirconia coatings deposited by plasma spraying. In order to properly assess the influence of the nanostructure, conventional and nanostructured coatings were produced and examined. Microstructural examination revealed that the nanostructured coating possessed higher microhardness and density and lower porosity level in comparison with the conventional coating. Also, tribological testing using block-on-ring arrangement yielded that the nanostructured coating possessed lower coefficient of friction in comparison with the conventional coating. Both coatings experienced an increase in the coefficient of friction as the sliding distance increased. Furthermore, the friction coefficient of both coatings linearly decreased with increasing load. Wear testing under light

load of 20 N resulted in abrasive wear of both coatings as a result of brittleness under low load. However, under high load conditions of 80 N, each coating exhibited different wear mechanisms. The nanostructured coating underwent plastic deformation under high load and formed smooth worn surface. Also, as a result of fatigue fracture, microcracks parallel to the sliding direction existed. On the other hand, the conventional coating wear mechanism was characterized as discontinuous wear tracks, which was an indication that the degree of plastic deformation of the conventional coating was less than that of the nanostructured coating. The superiority of the tribological properties of the nanostructured coating was a result of the preferable microstructure. Since the nanostructured coating consisted of smaller particles, the feedstock was more effectively melted resulting in enhanced cohesion among the coating splats, which in turn improved the wear resistance and microhardness. On the contrary, the increased size and level of porosity in the conventional coatings acted as stress concentration points, which resulted in lower wear resistance and inferior tribological properties.

2.3 Effects of Heat Treatment on Nanostructured Coatings

Park et al. [20] examined the mechanical properties and microstructure evolution of the nanostructured WC-Co coatings fabricated by detonation gun spraying with post heat treatment process. Two different spray parameters were used to produce the workpiece. The workpiece were, then, heat treated in an Ar environment at temperatures up to 900 °C. Using Vickers indentation testing, it was evident that the heat treatment up to 900 °C increased the microhardness due to the presence of η -carbides. On the other hand, an increase in fracture toughness and wear resistance was achieved by heat treatment up to 800 °C, but it decreased after heat treatment at 900 °C. The decrease of fracture toughness and wear resistance at temperatures above 800 °C was due to the growth of carbides by several hundred nanometers.

Wang et al. [21] examined the thermal shock behavior of nanoconstructed and conventional Al₂O₃/13 wt% TiO₂ coatings applied by plasma spraying. Three types of coatings were produced: one produced from conventional commercially available powder and the other two types were derived from the nanoconstructed agglomerated feedstock powders. Compared with the conventional coating, the nanoconstructed coatings had improved bonding strength and microhardness. In addition, thermal

shock resistance was much higher in the nanoconstructed coatings, which was related to the unique microstructure consisting of three-dimensional net or skeleton-like structure.

Lima and Marple [22] examined the properties and effects of nanoconstructed yttria stabilized zirconia (YSZ) thermal barrier coatings engineered to counteract sintering effects. Since YSZ was used as thermal barrier coatings in the hot section of gas turbines, heat treatment of the workpiece at 1400 °C for 1, 5 and 20 hours was carried out. It was noticed that the nanoconstructed coating had bimodal distribution in the micro structure as a result of the previously molten and resolidified YSZ particles as well as the previously semi-molten porous nano YSZ agglomerates embedded in the coating during the spray process. As a result of higher surface area in the nanoconstructed coatings and different sintering rates, it was found that the porosity level increased after 20 hours of heat treatment at 1400 °C to be 3.5 times the porosity level of the conventional coating. The different sintering rates and porosity level in the nanoconstructed coating prevented the increase of elastic modulus and thermal diffusivity over the time when subjected to elevated temperatures.

Rabizadeh et al. [23] investigated the effects of heat treatment on the properties of Nickel Phosphorus (Ni-P) electroless nano-coatings. When the heat treatment was carried at 200 °C, it was noticed that the hardness decreased as a result of hydrogen embrittlement and internal stress relieving. However, increasing the temperature of heat treatment to the range of 200 °C - 600 °C yielded significantly higher hardness values. Precipitation of nickel phosphides (Ni₃P) was anticipated to be the major factor for the increase in hardness. Furthermore, the corrosion resistance increased with heat treatment of the workpiece at 600 °C.

Yu et al. [24] examined the thermal stability of nanostructured 13 wt% Al₂O₃-8 wt% Y₂O₃-ZrO₂ thermal barrier coatings. The coatings were produced using air plasma spray onto stainless steel substrates. It was found that the increased annealing treatment time from 25 to 300 h resulted in increased ZrO₂ grain size from 63 to 120 nm. Furthermore, the presence of nano-sized Al₂O₃ formed intragranular structure that constrained the grain boundaries of ZrO₂ and inhibited its growth. In addition, sintering at 1100 °C for 300 h resulted in reduced porosity as a result of the grain growth and precipitation of Al₂O₃.

Kim et al. [25] examined the effects of post-spraying heat treatment on wear resistance of WC-Co nanocomposite coatings. The coatings were

produced using the high velocity oxy-fuel thermal spray process. Consequently, heat treatment was carried out at temperatures in the range of 400 – 1000 °C. Prior to heat treatment, XRD results indicated that the coating mainly consisted of WC and W₂C. Heat treatment in the range of 400 – 600 °C did not result in phase transformation and did not influence the wear resistance. On the other hand, heat treatment in the range of 600 – 800 °C resulted in phase transformation from WC and W₂C to η - carbides such as (W,Co)₁₂C and (W,Co)₆C. Furthermore, the wear resistance increased by 45% and the microhardness increased as well. On the contrary, heat treatment at 1000 °C resulted in complete transformation of WC to η -carbides and metallic W. Also, the coating surface experienced significant cracking as a result of the elevated temperature.

The effects of heat treatment of thermal barrier coatings were investigated by Wang et al. [26]. The yttria stabilized zirconia (YSZ) (8% Y₂O₃ partially stabilized zirconia) coatings were produced using air plasma spray. Following the coating process, heat treatment was carried out at temperatures ranging 600-1150 °C for periods ranging 15-300 h. An increase of grain size from 57 to 88 nm was observed as the annealing temperature increased. Also, the grain size increased from 57 to 188 nm

when the annealing time was increased. Furthermore, a low activation energy was observed in the study. The existence of micro pores and the grain-rotation-induced grain coalescence mechanism were the reasons behind the low activation energy.

2.4 Comparison Between Properties of Microstructured and Nano Structured Coatings

Cho et al. [27] conducted a study on HVOF coatings of micron and nano WC-Co powders. It was concluded that both the micron and the nano WC-Co had high hardness, which was desirable in sliding machinery applications. Furthermore, the nano sized powders yielded lower hardness than the micron sized powders, as a result of the increased decomposition of WC to W₂C, due to the larger specific surface area. On the other hand, the increased decomposition of WC in the coating produced by the nano sized powder resulted in lower friction coefficient. In addition, the decomposed graphite in the nano sized powder reacted with oxygen and formed carbonic oxide gasses that resulted in increased porosity in the coating, when compared with the coating that was produced using the micron sized powder.

Conventional air plasma spray and high velocity oxy-fuel titania (TiO₂) coatings as well as nanostructured HVOF TiO₂ coatings were examined

by Lima and Marple [28]. The nanostructured HVOF coating possessed 60% lower volume loss in the abrasion test and 65% increased bond strength when compared with the conventional coatings produced by air plasma spray and high velocity oxy-fuel. The improvement of the nanostructured HVOF coatings compared to the conventional APS coatings was a result of the lower porosity as well as the distribution of agglomerated nano particles. Even though all coatings exhibited similar hardness values, the nanostructured HVOF coating had the highest crack propagation resistance. The dense isotropic-like structure with randomly dispersed zones acted like crack arrestors by branching or blunting the crack tips, which increased the crack propagation resistance.

The fatigue and mechanical properties of nanostructured and conventional titania (TiO_2) thermal spray coatings were examined by Ibrahim et al. [29]. The low-carbon steel workpiece that were coated with nanostructured titania exhibited fatigue strength that was significantly higher than that of the workpiece coated with conventional titania. The presence of semi-molten nanostructured TiO_2 particles acting as crack arrestors was anticipated to be the reason behind the superior crack propagation resistance in the nanostructured coatings. Furthermore, the

fatigue life of the nanostructured coating was enhanced, due to the increased crack propagation resistance.

The microstructures and properties of thermal barrier coatings produced by plasma spray of nanostructured zirconia have been examined and compared with the conventional thermal barrier coatings by Tong et al. [30]. The plasma sprayed nanostructured Zirconia thermal barrier coating had improved combined strength and thermal shock resistance compared to the conventional thermal barrier coatings of magnesia and yttria stabilized zirconia. The improvement was because of the formation of close packed structure, small cavities and laminar structures. In addition, the nanostructured coating exhibited oxidation resistance higher than that of ceramic surfaces.

A comparison of the thermal shock behavior between plasma-sprayed nanostructured and conventional zirconia thermal barrier coatings has been conducted by Chun-bo et al. [31]. The thermal shock resistance of nanoconstructed thermal barrier coatings was superior to that of the conventional coatings. Furthermore, the thermal shock life of the nanoconstructed coatings decreased as the test temperature increased. Both TBCs, nanostructured and conventional, failed by spalling at the coating interface as a result of the thermal shock testing. The constituent

phases of the as sprayed TBCs produced by the nanostructured and conventional feedstock remained the same without phase transformation after thermal shock testing.

2.5 Effects of Coating Process Parameters of Nanostructured Coatings

Thermal spray coatings directly depend on the spray parameters and feedstock material. However, in several cases, the resulting coatings do not match the theoretically expected results, due to particle disintegration during the spray process. As a result, Fogarassy et al. [32] examined the agglomerated nanostructured particles disintegration during plasma thermal spraying process. Numerical analysis, calculations and finite element analysis were performed to determine the thermal field velocity distribution in the plasma jet. It was found that particles with 100 μm diameter that were close to the axis of the plasma jet exploded before complete melting by 0.3 ms. Furthermore, particles projected within 50 of the plasma jet axis disintegrated by exploding before impacting the substrate. On the other hand, Since the quality of the coatings depended on the deposited layers morphology, utilizing nanoconstructed feedstock preserved the nanostructure of the deposited coatings, which maintained the desired quality.

When certain thermal spray coating properties, such as maintaining nanostructures, are desirable, different variables must be considered. One of the variables, which was examined by Lau et al. [33], is the particle behavior during high velocity oxy-fuel thermal spray. Flake shaped agglomerates were produced via mechanical milling in methanol and liquid nitrogen environments. It was found that the particle velocity profile was dependent upon the particle thickness. Furthermore, the thickness of the particles was a function of the milling media. In that case, methanol milled particles were more efficient in comparison with cryomilled agglomerates which had 75% larger thickness.

The influence of particle temperature and velocity on the microstructure and mechanical behavior of high velocity oxy-fuel (HVOF)-sprayed nanostructured titania coatings have been assessed by Gaona et al.[34]. To properly assess their influence, several particle temperatures and velocities were employed. It was observed that the particles temperatures and velocities linearly increased as the propylene flow rate was increased. Furthermore, the highest temperatures and velocities were achieved at the richest air/fuel ratio condition. Also, the coatings produced using the highest temperature and velocity exhibited isotropic-like structure with decreased porosity level. In addition, using the Almen strips, it was

evident that the residual stresses were higher in the coatings produced with higher particle temperature and velocity. The increased stress was a result of the increased peening effect due to the increased velocity. Also, the stress level increased with increased temperature as a result of greater particle shrinkage upon solidification on the substrate during the coating process. Other effects of the increased particle velocity and temperature included increased presence of anatase structure, same as feedstock, due to semi melting the particles, which in turn enhanced the coating bond strength. Also, the increased particle temperature resulted in enhanced intersplat contact, increasing the cohesive strength and the microhardness.

The effects of plasma spray parameters on the microstructure and properties of nanostructured coatings were investigated by Shaw et al. [35]. It was found that the effect of the spray parameters on the nanostructured coatings was similar to that on the microstructured coatings. All spray parameters had effect on the produced coatings, however, the most influential parameter was the ratio of electrical power to the primary argon gas flow rate ($I.V/Ar$). Depending on the $I.V/Ar$, different spray temperatures were achieved, which resulted in different coating phases. In addition, changing the ratio of electrical power to the

primary argon gas flow rate greatly influenced the hardness and wear resistance, as a consequence of the different coating densities.

Lima et al. [36] from the State University of New York evaluated the microhardness and elastic modulus of thermally sprayed nanostructured zirconia coatings. By selecting three different power levels, two argon flow rates and two spray distances, a relationship between microhardness, elastic modulus and surface roughness with certain trend was noticed. Smoother coatings exhibited increased microhardness and elastic modulus and vice versa for all spray parameters. Higher degree of splat flattening was correlated with the decrease in surface roughness. The increased flattening resulted in increased contact between the splats, which in turn enhanced the coating cohesion. Consequently, the microhardness and elastic modulus increased with the enhanced coating cohesion. With such relationship between the roughness, microhardness, and elastic modulus, a surface profilometer could be used to assess the microstructural properties of the coatings in-situ.

Marple et al. [37] examined the effects of fuel type on the HVOF WC-12Co cermet coatings. Kerosene, hydrogen and propylene were used as gun fuel to produce the coatings. The highest particle jet temperature was achieved using propylene as fuel and the lowest was achieved using

kerosene. On the other hand, for a given temperature, the highest particle velocity was achieved using kerosene fuel and the lowest velocity was achieved using propylene fuel. Efficiency assessment yielded that the most efficient thermal spray process was achieved when hydrogen was used as fuel. It was observed that the increased particle temperatures and velocities yielded coatings with increased hardness and lower porosity. Degradation of the carbide phase by formation of W phase was observed in coatings produced by the different fuels. However, the higher temperature and lower velocity characteristics of using propylene as fuel resulted in the highest carbide degradation.

2.6 Summary of Literature Review

Microhardness, wear resistance, shock resistance, surface roughness, and porosity levels of nanostructured coatings were considered as critical properties, which are affected by the feedstock material characteristics and process parameters. The literature studies, that were presented in the past, have greatly contributed to the development of nanostructured coatings, in an effort to achieve optimum properties. Furthermore, several studies included the effects of post coating heat treatment to simulate the influence of elevated temperature environments, such as combustion components of gas turbines. The main focus of the studies presented in

the open literature is to assess the properties of thermally sprayed coatings and the influence of process parameters and heat treatment on the resulting coating characteristics. However, no comprehensive study is found in the open literature to introduce comparative evaluation of the influence of nanoparticles, when added to the feedstock of thermal spray and welding coating processes. Furthermore, some studies in the open literature show contradicting results regarding the influence of nanoparticles on the microstructural, mechanical and tribological properties. This issue is addressed in the thesis work through examining the influence of nanoparticles in thermal spray and welding feedstock on the metallurgical properties of the resulting coatings.

Chapter 3 – Experimental Equipment & Procedures

3.0 Introduction

Experiments were conducted to examine the metallurgical properties of coatings onto carbon steel (AISI-1020) which were produced from conventional feedstock and feedstock that was blended with nano particles. The experiments include workpiece preparation, gas metal arc welding overlay coatings, wire arc spray coatings, heat treatment, and measurement of hardness.

3.1 Specimen Design

The majority of rotating equipment components at Saudi Aramco and other oil producing companies, which suffer from wear, erosion, and deterioration as a result of operating at elevated temperatures are made of low grade carbon steel, such as AISI-1020. Other rotating equipment components, which are made of high strength materials and superalloys, are typically designed to withstand the harsh service environments. Therefore, they do not require advanced surface treatment or surface enhancements. As a result, both workpiece groups for gas metal arc welding overlay coating as well as wire arc spray are made of AISI-1020 carbon steel. Furthermore, heat treatment of the wire arc sprayed

workpiece is considered to simulate the effects of high temperature on the coating microstructure and properties.

3.2 Gas Metal Arc Welding

The welding overlay coating consumable materials and process details are as follows.

3.2.1 Gas Metal Arc Welding Feedstock

Two welding feedstocks were utilized, conventional GMAW feedstock, and nano-structured GMAW feedstock.

3.2.1.1 Conventional GMAW Feedstock

Conventional electrode wire is used to build up material similar to that of the substrate. The solid wire is copper plated to prolong the wire life and to enhance the electrical conductivity for maintaining stable arc during application. The elemental composition of wire material is given in Table 3.1.

Table 3.1. Chemical composition of conventional wire material [wt.-%].

C	Si	Mn	P	S	Cu	Fe
0.11	0.53	1.15	0.011	0.012	0.14	Balance

3.2.1.2 Nano-structured GMAW Feedstock

Welding consumables EnDOTec continuous electrodes are compatible with most conventional, constant voltage power sources [38]. The nanostructured wire (DO*390N) is ideal for maintenance and repair applications or batch manufacturing where highest integrity welding, efficiency and productivity are required. It provides outstanding abrasion and erosion resistance performance like tungsten carbide without using scarce exotic elements. The elemental composition of wire material is given in Table 3.2.

Table 3.2. Chemical composition of nano-structured wire material [wt.-%].

C	Si	Mn	Cr	Mo	Nb	W	B	Fe
1.34	0.46	0.22	15.43	3.71	4.18	7.84	4.18	Balance

The slag-free deposit contains a high volume fraction of ultra-hard, complex borocarbides uniformly distributed within an iron alloy matrix. The unique nanoscale type microstructure ensures exceptional performance against wear by severe abrasion & erosion retaining elevated bulk hardness properties to 750°C. Weld deposit exhibits stress relieving microfissures, smooth ripple-free weld surface contour, grindable, slightly magnetic deposit, low coefficient of friction without lubrication

and unique peripheral arc characteristics. Low heat input for minimal dilution ensures best possible weld layer properties and maximized weld metal recovery [38].

3.2.2 Gas Metal Arc Welding Process

To deposit the nanostructured wire, feed arc welding equipment was used in accordance with the American National Standards for Arc Welding Equipment (ANS/IEC 60974-2009). Models with programmable, pulsed arc, metal transfer modes offer optimal performance. The welding was achieved using the electrode at an angle of 70-80°. This provided clean, spatter-free, high profile weld deposits. To achieve sufficient weld deposition at the surface of the workpiece, the multi-passes of welding were carried out while the initially deposited weld was still hot. The shielding gas mixture was used during the deposition (97.5% Ar and 2.5% CO₂). Welding parameters are given in Table 3.3.

Table 3.3. Welding parameters.

Wire Diameter (mm)	Voltage (V)	Current (A)
1.6	23-34	170-300

3.3 Wire Arc Plasma Spray

The wire arc plasma spray process and consumables are the following

3.3.1 Wire Arc Plasma Spray Consumables

Similar to the coatings produced by GMAW, two consumable wire materials were incorporated; conventional and nano-structured wire feedstock materials.

3.3.1.1 Conventional Wire Arc Plasma Spray Feedstock

The conventional wire material used for wire arc spray, TAFA 95MXC, is specifically made to be used for this process. It is intended to produce hard coatings that are corrosion and abrasion resistant, while maintaining acceptable coating elasticity. Coating thickness of 0.010 inches to 0.060 inches is achievable using this wire material. The elemental composition of the consumable wire is given in Table 3.4.

Table 3.4. Chemical composition of conventional wire material [wt.-%].

Si	Cr	Mn	B	Fe
1.6	29.0	1.65	3.75	Balance

3.3.1.2 Nano Structured Wire Arc Plasma Spray Consumables

Commercially available TAFA 140MXC nano-structured arc spray wire is utilized to produce coated workpiece. Consisting of nanocrystalline and amorphous phases, the resulting coatings are expected to possess unique properties. High hardness, wear and corrosion resistance as well as low porosity are expected coating properties based on the wire element composition shown in Table 3.5.

Table 3.5. Chemical composition of nano-structured wire material [wt.-%].

Cr	B	Mo	W	Mn	C	Nb	Si	Fe
<25	<5	<6	<15	<3	<4	<12	<2	Balance

3.3.2 Wire Arc Plasma Spray Process

Wire arc plasma spray offers desirable characteristics over other coating or overlay processes such as gas metal arc welding. The improved characteristics include fast deposition rate, easiness of operation, consistency of results and minimal heat affect to the substrate material. A total of fourteen workpiece were produced; seven workpiece of different coating thicknesses using the conventional wire material and seven workpieces of different coating thicknesses using the nano-structured

wire material. The spray parameters, shown in Table 3.6, were fixed for all of the workpieces. However, the number of passes is varied to produce different coating thicknesses.

Table 3.6. Wire arc plasma spray parameters.

Voltage (V)	Head Pressure (psi)	Step Size (in)	Current (A)	Primary (psi)	Second (psi)	S.O. (in)
33	45	8.8	150	67	67	4

3.4 SEM, EDS and Optical Microscope

Cross-section and surface photomicrographs of the workpieces were obtained using JEOL JDX-3530 LV scanning electron microscope (SEM). With resolution of 3.0 mm, magnification of x5 to 300,000 and accelerating voltage of 03 to 30 kV, the desired SEM results could be accurately achieved. On the other hand, the elemental analysis was carried out using energy dispersive spectroscopy (EDS). Figure 3.1 is a picture of the SEM equipment.



Figure 3.1. Scanning Electron Microscope model JEOL JDX 3530 LV.

Surface micrographs and microscopic observations were conducted using an optical microscope that was manufactured by Olympus. The Olympus BX 60 optical microscope is combined with a digital microscope camera (DMC) manufactured by Polaroid. Five magnification levels of 50X, 100X, 200X, 500X and 1000X are achievable using the Olympus microscope. In order to switch between the magnification levels, the microscope has a revolving nosepiece, which contains five lenses that correspond to the magnification level.

3.5 X-ray Diffraction (XRD)

Mo-K α radiation is used through Bruker D8 Advance unit for XRD analysis with typical settings of 40 kV and 30 mA. Because of the penetration depth Mo-K α radiation into the coating, in the range of 10 –

20 μm , the residual stresses measured using XRD provided data regarding the surface region of the workpieces. Table 3.7 and figure 3.2 illustrate the specifications and show a picture of the XRD machine respectively.

Table 3.7. XRD machine Specifications.

Model	AXS D8 Bruker Inc
Sample Positioning & Rotation	Goniometer; Eulerian Cradle; Theta-Theta, Theta-2Theta
X-Ray Source & Optics	Collimeter or slits to reduce angular divergence of the incident beam
Performance Specifications	2-Theta Angular Range (degree) 110 to 168 Peak Count Rate (cps) 2.00E6 Max Sample Dia (mm) 600 Computer based interface and display; Other digital or analog interface display; Ability to process and analyze the diffraction data



Figure 3.2. X-ray Diffraction model Beuker D8 Advance.

3.6 Indentation Tests

An Indentation Hardness Tester manufactured by BUEHLER Com, Figure 3.3, was utilized to perform the tests. Optical microscopy was performed to visualize the cracks around the indentation mark, which was formed using 20 N load level. Indentation tests at the coatings, coatings-substrate interface and at the substrate were performed at 20 different locations to properly and accurately assess the properties.



Figure 3.3. Indentation Hardness Tester manufactured by BUEHLER Com.

3.7 Heat Treatment

All the workpieces produced by wire arc spray were heat treated using a synchronous atmospheric heat treatment oven. The heat treatment was carried out at 800 °C for five hours, then the samples were left to cool at ambient temperature, without forced convection or quenching. In general, some components of rotating equipment, such as gas turbines, operate at around 800 °C. To resemble such conditions, the heat treatment temperature was selected as 800 °C. Also, treatment time of five hours ensures that the effects of that temperature, if any, take place.

Chapter 4 – Results and Discussions

4.1 Coating Produced by Deposition of Nano Particles Blended Wires

Coating of carbon steel surface with welding deposition pertinent to repair applications is carried out. Two welding wires are used to deposit the coating material onto the base material surface through electrical arc welding method. Optical microscopy and SEM are carried out for microstructural analysis.

Figure (4.1) shows optical micrographs of top surface of the workpiece. It is evident that no surface crack due to thermal effects is observed. In addition, no cavitation and voids are formed due to excessive heating during the multi-passes deposition. The melt tracks reveal that the overlapping ratio is about 90%, which provides a continuous melt deposition at the surface. However, the melt tracks are set slightly apart during the deposition process. This provides smooth deposition without irregular surface texturing while avoiding excessive temperature rise during the deposition process. The nominal thickness of the coating layer is in the order of 5 mm, which is usually the case for the repair applications. The oxide formation at the surface is evident through the coloration of the coating. This is also revealed from the EDS analysis as

shown in Figure (4.2). The oxide formation is associated with the initial oxidation of the workpiece surface prior to the deposition process. In this case, during the deposition process, oxygen may release from the workpiece at high temperature and undergoes an exothermic reaction at the melt surface. Since the amount of oxygen is less, the degree of oxidation is also less at the surface, i.e. no loose debris is observed during and after the process.

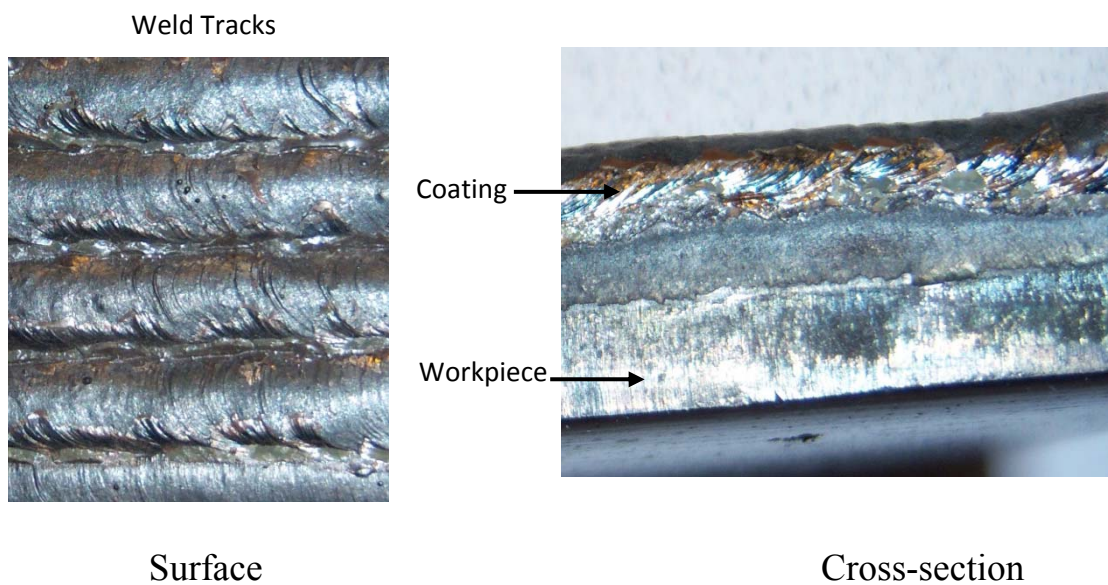


Figure 4.1. Optical micrographs of coating surface and cross-section.

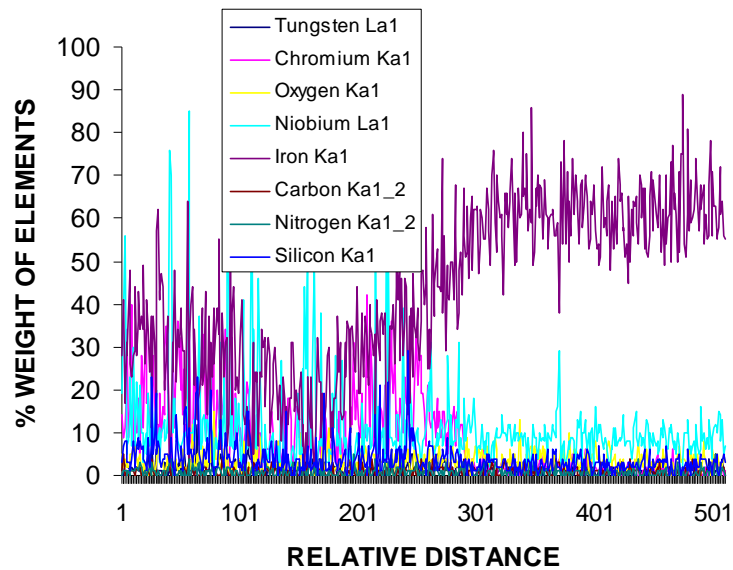


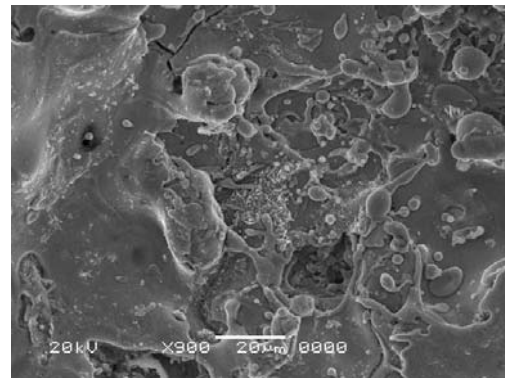
Figure 4.2. EDS line scan for elemental composition of coating.

Figure (4.3) shows SEM micrographs for the cross-sections of both coatings produced by conventional (micrographs (a), (b) and (c)) and the nano-particle blended electrodes (micrographs (d), (e) and (f)). It is evident from SEM micrographs that there is no discontinuity in terms of cavitations at the interface between the coating and the base material. This is true for coatings produced by nano-structured and standard electrodes. In addition, no microcracks due to high temperature gradients in the vicinity of the interface are observed. This shows that the coating rate is not significantly high causing the excessive thermal stresses in this region. However, the microstructure developed in the coating is completely different than that of the base material. This is particularly true for nano-particle blended coating. In this case, the nano-particles

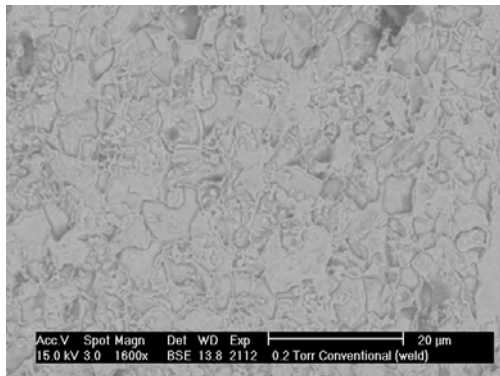
remain almost undissolved in the metallic matrix. In some regions, small grains are observed where the nano-particles are concentrated. This may occur during the deposition process, in which case, some of nano-particles, such as WC remains in solid phase and these particles may agglomerate locally. It should be noted that nano-structured zones act as crack arrests [39]. The crack tends to propagate through the coatings weakest link and cracks propagating and reaching these well-embedded regions tend to be arrested by the nano-structured zones.



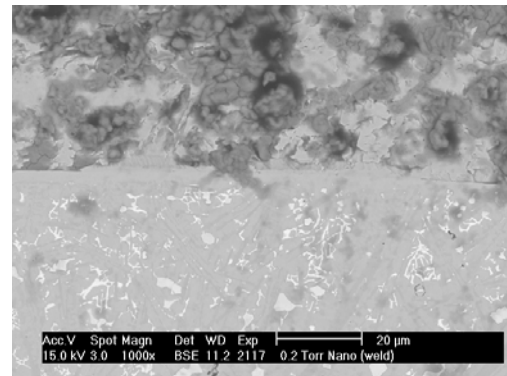
(a) Conventional Wire (SEM)



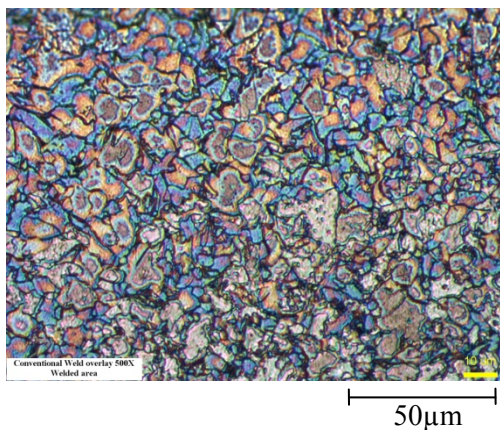
(d) Nano-structured wire (SEM)



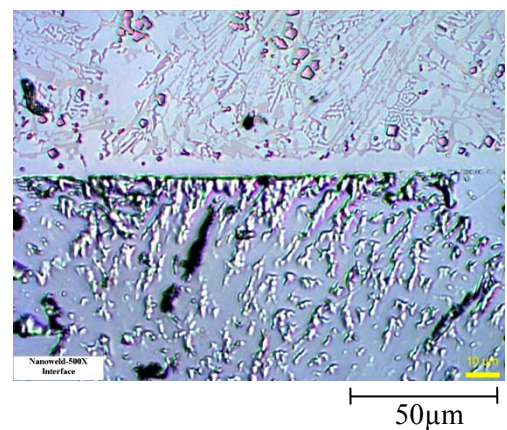
(b) Conventional Wire (SEM)



(e) Nano-structured wire (SEM)



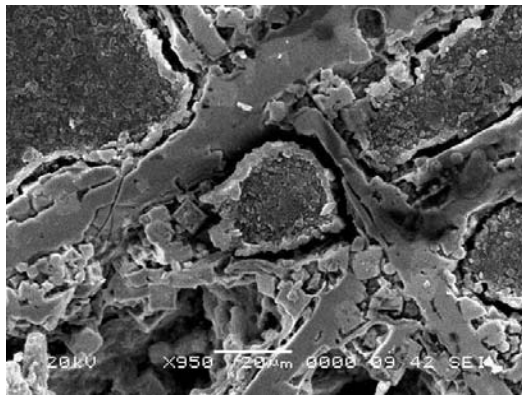
(c) Conventional Wire (Optical)



(f) Nano-structured wire (Optical)

Figure 4.3. SEM and optical micrographs of conventional and nano-structured coating cross-sections.

Figure (4.4 micrographs (a) and (b)) shows close view for the cross-sections of the nano-structured coatings. The structure involves small grains and crystalline materials. In this case nano-particle interacts with the grain boundary to reduce the energy of the boundary particle system and restrains the boundary movement [39]. Moreover, during the grain growth the area for the nano-particles is reduced. This results in enhancement of nano-particles concentration locally in the metal matrix. This is true for nano-particles having high melting temperatures. Moreover, the presence of conventional nano-particles in the matrix can prevent grain growth through slowing down the growth kinetics via reducing the boundary free energy or the grain boundary mobility. Moreover, the clustered nano-particles act as inclusion in the matrix suppressing the grain growth nearby until the particles dissolve or become mobile in the molten state of the matrix. The nano-structures, composing of nano-particles, generate large number of internal interfaces in the liquid matrix causing the formation of small grains. This occurs locally while resulting in randomly distributed fine grains in the structure.



(a)



(b)

Figure 4.4. SEM micrographs of cross-sectional views of nano-structured coating.

Table 4.1 shows microhardness measurement results while figure 4.5 shows the indentation marks at the surface. Microhardness measurements reveal that hardness of the coating increased as compared to the base material, which is carbon steel. The increase in the hardness is because of the melting and resolidification processes during the coating deposition. In this case, fine grain structures are responsible for increase in hardness. In the case of nano-structured electrode, microhardness increases significantly in the coating. In this case, the hardness ratio of coating to base material is about 5.5. This is because of the fine grain structured formed in the coating due to presence of the nano-particles. Consequently, grain refinement and compact structured due to nano-particles concentration at grain boundaries are responsible for increased hardness in the coating. In the case of interface between the coating and

the base material, hardness gradually decreases in the coating towards the interface while it increases towards the interface in the base material. This indicates that the variation in the coating due to differences in the thermal conductivities of coating and the base material is responsible for this behavior. Moreover, it is evident from the optical picture of the indentation marks that the crack does not form around the marks. This indicates that the coating is still ductile despite the hardness is high.

Table 4.1. Microhardness of the coating and the base material.

	Nano-structured Coating	Standard Coating	Base Material
Microhardness (HV)	950	450	130

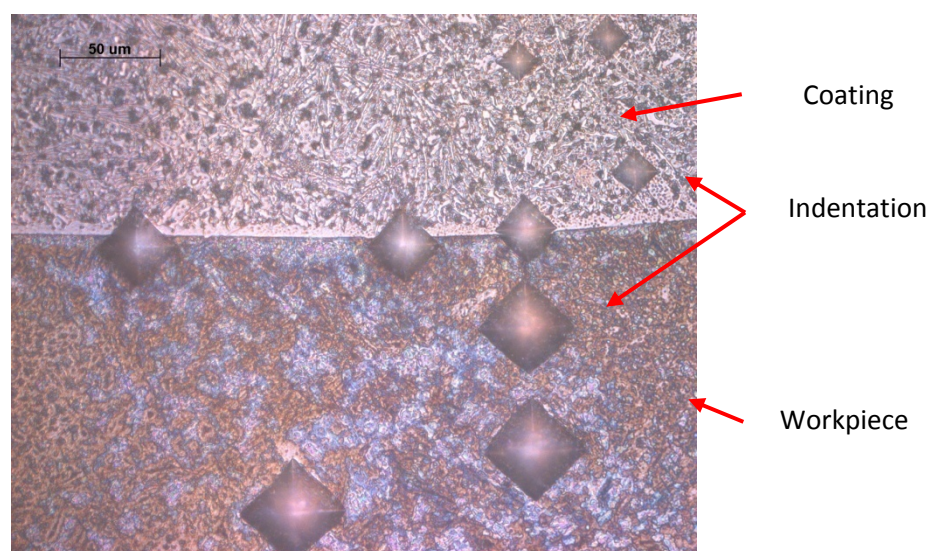
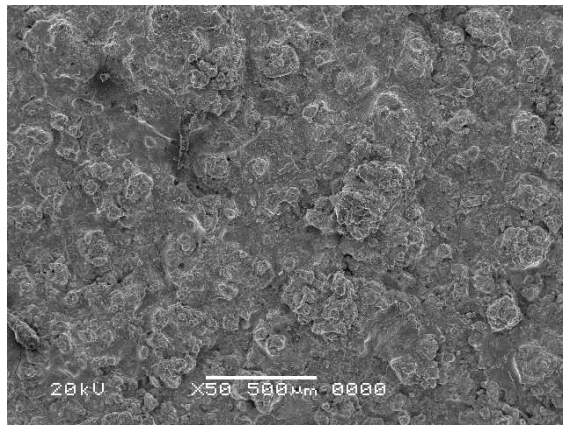


Figure 4.5. Optical micrograph of cross-sectional view of nano-structured coating and indentation marks.

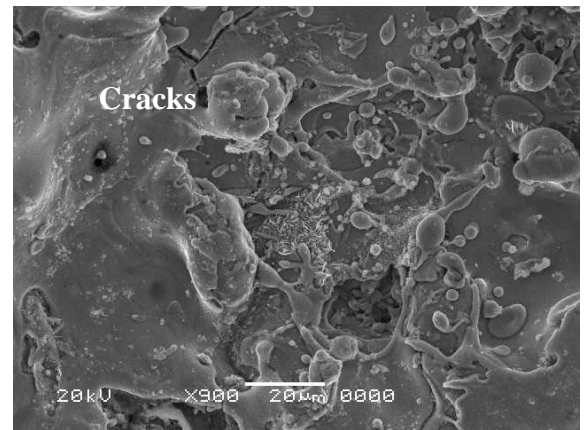
4.2 Wire arc sprayed nanostructured coatings

Arc spraying of the nanostructured wire onto carbon steel surface is carried out. The morphological and microstructural changes in the resulting coatings are examined. The study is extended to include the heat treatment of the coating. In addition, hardness of the coating prior to and after the heat treatment is measured.

Figure (4.6) shows SEM micrographs of the top surfaces of the wire arc spray coating prior to heat treatment (micrographs (a) and (b)) and post heat treatment (micrographs (c) and (d)). It is evident that the surface is free from the large cavities and cracks, provided that the hilly morphology due to dimples results in high surface roughness.

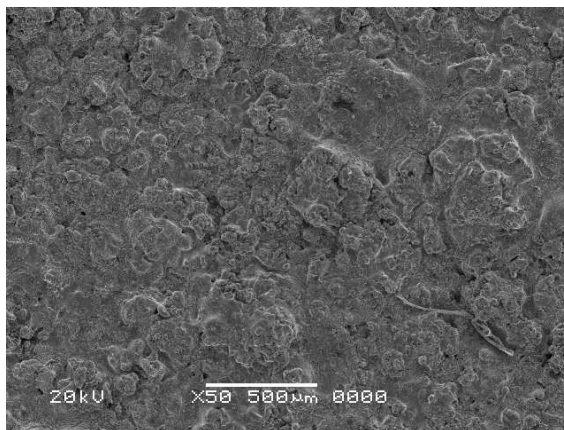


(a)

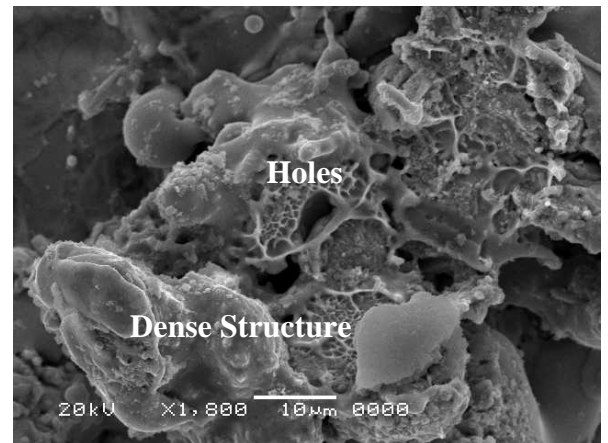


(b)

Prior to Heat Treatment



(c)



(d)

After Heat Treatment

Figure 4.6. SEM micrographs of top surface of arc sprayed coating prior and after the heat treatment process.

This can also be seen from the surface texture profile, which is shown in figure (4.7). It can be observed that the surface roughness is in the order of 15 μm , which is considerably high as compared to other coating methods [40]. However, no loose or partially loose particles are found at the coating surface. The closed examination of the surface texture reveals

Since the nano particles contain WC, they appear as the sub-micron fine grains in the surface region. However, due to high temperature involvement during the spraying process, some of the carbides undergo the oxidation reaction in the surface region. In this case, WC reduces to W_2C and a carbonic gas is formed [41]. This can also be seen from XRD diffractograms, which is shown in Figure (4.8). This results in micro-sized holes or cavities at the surface. This situation is observed from SEM micrograph. The presence of the dense layer around the micro cavities reveals the presence of carbides in this region.

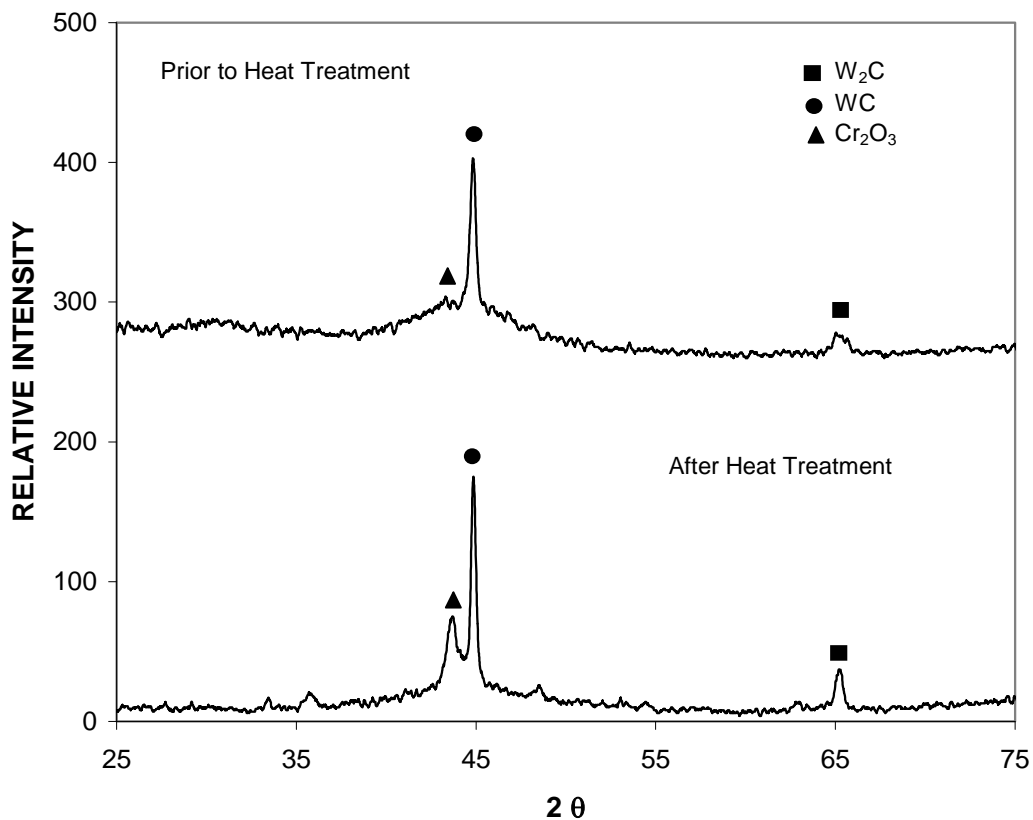
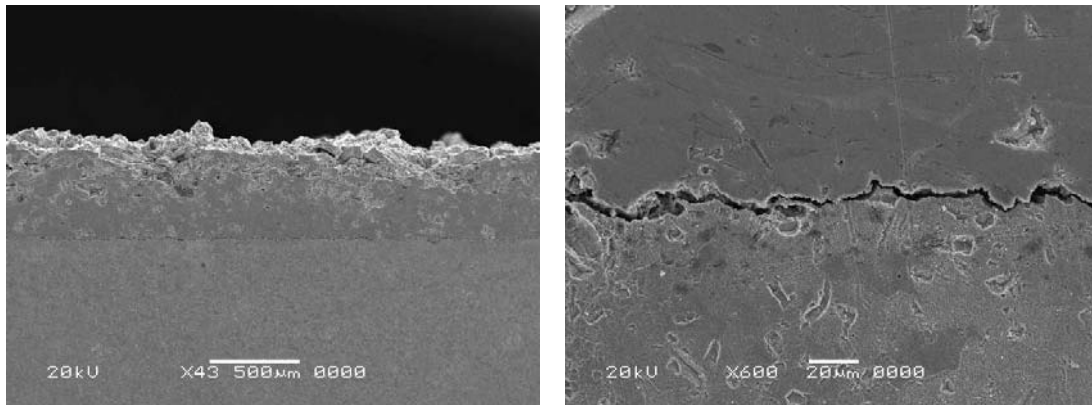


Figure 4.8. XRD Diffratogram for coating prior and after heat treatment.

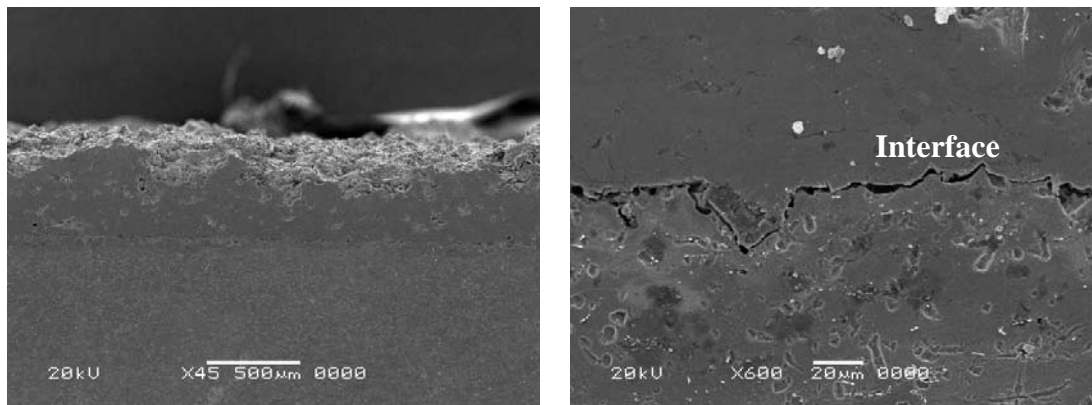
Figure (4.9) shows SEM micrograph of cross-sections of coating and the base material prior to heat treatment (micrographs (a) and (b)) and after the heat treatment process (micrographs (c) and (d)). It is evident that arc spraying produced almost uniform coating at the workpiece surface. No clear lamellar structure is observed unlike the other coating techniques. The continuous line of separation is evident at the coating interface for heat treated and untreated workpieces. This is attributed to the thermal expansion of the base material and the coatings at different rates. Consequently, this develops extended cavity formation across the interface at the end of the cooling cycle. In the surface region, particles oxidized appear as dark inclusions in the coating. This is particularly true in the vicinity of the surface. It should be noted that oxidation causes the particles size and mass to increase; therefore, small voids are formed in the vicinity of the oxidized particles.



(a)

(b)

Cross-section of Coating Prior to Heat Treatment



(c)

(d)

Cross-section of Coating After Heat Treatment

Figure 4.9. SEM micrographs of cross-section of the workpieces prior to and after heat treatment.

The formation of oxides in the liquid melt can cause heterogeneous nucleation sites. Once the nucleation starts, crystallization is fast and under cooling during the crystallization causes formation of phases, which are several orders of magnitude larger than the nano-particles. This situation is observed in the surface region of the coating. Moreover, the presence of semi-molten particles during the spraying causes small

cavities in the coating, provided inter-connected small cavities or pores is not observed. The close examination of the SEM micrographs reveals that the nano-scaled particles remain as nano-sized with the presence of grain coarsening. This is associated with the very stable phase boundaries, which, in turn, results in the structures maintaining their sizes after the exposure to the heat treatment process. It should be noted that the tensile stress developed due to thermal expansion in the surface region during the heat treatment process causes coating failure from the local delamination and spalling. However, this situation is not observed in the coating, particularly in the coating base material interface. SEM micrographs also show that small grains are formed in the region where the un-dissolved nano-particles are concentrated. In this case, structures comprising of undissolved nano-particles generate large number of internal interfaces in the liquid matrix resulting in the development of the small grains. Table 4.2 gives the EDS results across the cross-section of arc coating prior to heat treatment in areas defined in Figure (4.10).

Table 4.2. EDS results across the cross-section of the workpiece.

Spectrum	O	Al	Cr	Fe	W
Spectrum 1	23.39	17.67	11.13	Balance	2.16
Spectrum 2	0.00	0.00	30.63	Balance	0.00
Spectrum 3	35.06	1.60	2.42	Balance	0.00
Spectrum 4	7.87	3.34	13.82	Balance	4.67
Spectrum 5	2.80	0.57	18.03	Balance	7.21
Spectrum 6	6.02	1.18	16.26	Balance	10.23
Spectrum 7	16.16	2.88	14.24	Balance	5.53
Spectrum 8	7.74	0.84	16.33	Balance	8.14
Spectrum 9	0.00	0.00	0.00	Balance	0.00
Spectrum 10	2.72	0.00	0.00	Balance	0.00

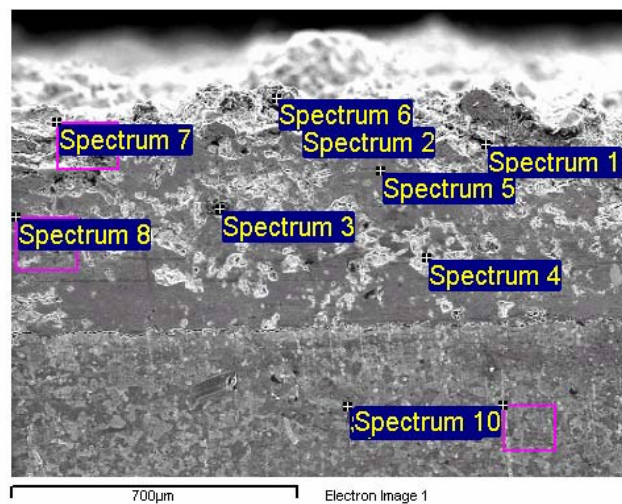


Figure 4.10. SEM micrograph for the cross-section showing EDS spectrums.

Table 4.3 gives microhardness results at the surface and at the cross-section of the coating prior and after the heat treatment process while Figure (4.11) shows the indentation marks in the coating and the base material, which is carbon steel. The microhardness attains high values at the surface as well as at the coating cross-section. This is associated with the fine grains and presence of fine structures comprising of nanoparticles. Moreover, the microhardness remains almost the same after the heat treatment process indicating the microstructural stability prior and after the heat treatment process. The hardness ratio of the coating to base material hardness is in the order of 4 times. This indicates the grain refinement and compact structures, which are responsible for the increased hardness. The optical image of the indentation marks reveals that no cracks are formed around the edges of the plastically deformed marks. Consequently, the residual stress level is low in the coating circumventing the crack formation under the applied indentation load.

Table 4.3. Microhardness results for the base material, arc sprayed prior and after the heat treatment process.

Base Material Hardness (HV)	210
Coating Hardness Prior to Heat Treatment (HV)	1100
Coating Hardness After Heat Treatment (HV)	800

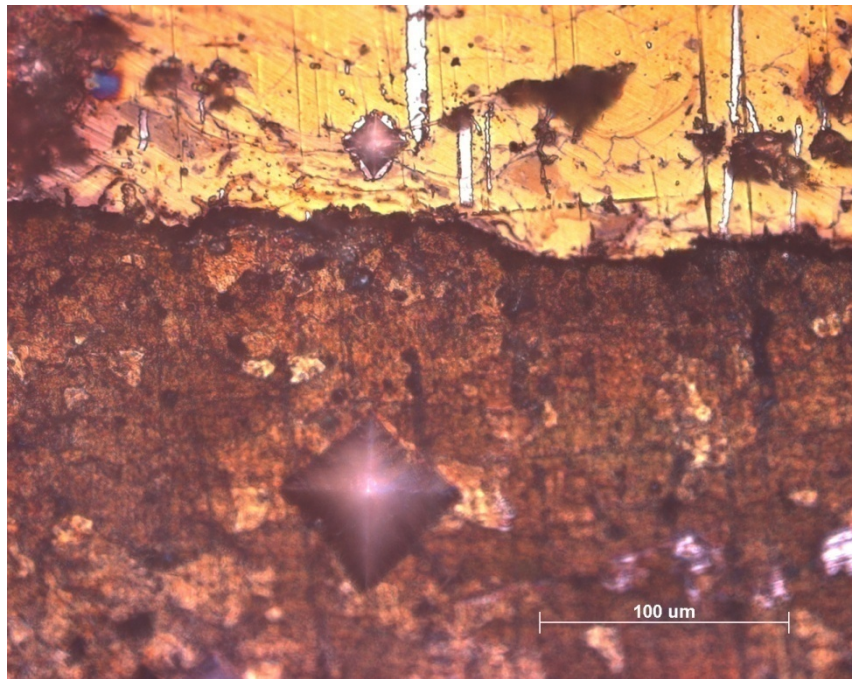


Figure 4.11. Indentation marks on the cross-section of the workpiece.

Chapter 5 – Conclusions and suggestions for future work

5.1 Coating Produced by Deposition of Nanoparticles Blended Wires

Welding deposition on to carbon steel sheet is considered for repair applications. The coating is realized using two types of wires, namely standard and nano-structured wires. The metallurgical changes and microhardness variation in the resulting coatings are examined. It is found that the coating was free from microcracks and voids. The presence of nano-particles in the coating suppresses the growth of grains during the solidification process. Consequently, dense structures with fine grains are resulted in the coating. In addition, the regions with high concentration of nano-particles act as crack arresting centers. Therefore, high stress levels developed in the cooling cycle may not result in cracks due to the presence of nano-sized particles in the coating. Nano-particles concentrated in some regions in the coatings; however, the concentrated regions are randomly distributed. This, in turn, results in large number of interfaces in the liquid matrix while suppressing the grain growth in this region. The microhardness tests reveal that microhardness of coating increases substantially for coating deposited using the nano-structured

wires. This is because of the grain refinement in the coating. The variation in the thermal properties across the coating base material interface causes variation in the hardness in this region. In this case, microhardness reduces towards the interface for nano-structured coating while microhardness increases towards the interface for the base material.

5.2 Wire Arc Sprayed Nanostructured Coatings

The coating through arc spraying of nano-structured wires is produced onto the carbon steel substrate. The morphological and microstructural changes in the coating is investigated using SEM and optical microscope. The influence of heat treatment on the morphology, microstructure , and microhardness of the coating is examined. It is found that no large cavities and cracks are observed at the surface of the coating. However, the formation of dimples like textures at surface increases significantly the surface roughness of the coating. The occurrence of the high surface roughness is attributed to the presence of semi-molten particles during the spraying process. The compact structures existing of nano sized particles are observed at the surface as well as in the coating. This is related to the presence of the carbide particles in the coating. Heat treatment does not notably modify the coating structure. However, the formation of locally oxidized particles in the surface region is evident. This appears as black

inclusions in the surface region. Moreover, the presence of oxidized particles causes partial delamination of the coating in the surface region. Oxidation of the molten or solid particles (such as carbides) during the spraying process results in the formation of the carbonic gases. This causes the formation of the small holes at the coating surface. The dense structure around these holes indicates the presence of the carbide particles in this region. The agglomeration of nano-sized particles in the coating suppresses the formation of large grains. Consequently, fine grains are formed in the region where the partially dissolved carbide particles are present. The microhardness of the coating attains significantly higher values as compared to the base material. This is attributed to the fine grains and the presence of compact structures consisting of nano-sized particles. Microhardness does not alter after the heat treatment process. However, the thermal expansion of coating and the base material at different rates causes elongated cavities across the coating-base material interface.

Suggestions for Future Work

In the present work, metallic coatings produced from feedstock materials that were blended with nano particles were examined. The coatings were produced using GMAW and wire arc spray processes onto carbon steel AISI-1020 substrates. SEM, EDS, XRD, microscopy and microhardness tests were performed. The testing and examination results indicated that the presence of nanoparticles increased the coatings hardness and suppressed the initiation and propagation of cracks. However, other material properties and the influence of the process parameters on erosion and wear resistance of the resulting coatings were not investigated. Consequently, the following studies can be recommended for the future work:

- Investigate the influence of coating thickness on coating properties. Since coatings with different thicknesses are produced, it is anticipated that there may be a relation between the coating thickness and material properties such as wear and corrosion resistance.
- Simulate the coating processes using numerical models. This will provide better understanding regarding the temperature distribution in the coating during the coating process. The theoretical model can be used to fine tune the process parameters to achieve optimum coating properties for the desired applications.

- Conduct Jet impingement tests. In this case, erosive environments of some rotating equipment such as pumps could be simulated to assess the material performance in such environments.
- Examine the wear properties of the coatings produced under different loads and at different conditions such as wet/dry ambients. The influence of size of the nano particles on the wear properties can be evaluated as well.
- Assess the corrosion behavior of the coatings produced, since the nano particles influenced the coatings structure such as increased compactness and reduced porosity.

References

- [1] N. Taniguchi, On the basic concept of nano-technology, intl. cong. Prod. London, part II, 1974.
- [2] J. R. Davis, Surface Engineering for Corrosion and Wear Resistance, 2001, Maney Publishing
- [3] http://www.faculty.rsu.edu/~clayton/kelicas/paper_files/image003.jpg
- [4] E. Oberg, F. D. Jones, H. L. Horton, H. H. Ryffel, Machinery's Handbook (28th Edition) & Guide to Machinery's Handbook, 2008, Industrial Press.
- [5] M. Bass, V. N. Mahajan and E. V. Stryland, Handbook of Optics Volume II, 2010, New York: McGraw-Hill.
- [6] http://www.advancedpowerwelding.com/images/welding_essentials05.gif
- [7] <http://www.firstscience.com/home/images/stories/articles/jet2.jpg>
- [8] H. Chen, G. Gou, M. Tu and Y. Liu, Characteristics of nano particles and their effect on the formation of nanostructures in air plasma spraying WC-17Co coating, Surface and Coatings Technology, 203, 2009, 1785-1789.
- [9] J. Kim, H. Yang, K. Baik, B. G. Seong, C. Lee and S. Y. Hwang, Development and properties of nanostructured thermal spray coatings, Current Applied Physics, 6, 2006, 1002-1006.
- [10] Y. C. Zhu, C. X. Ding, K. Yukimura, T. D. Xiao and P. R. Strutt, Deposition and characterization of nanostructured WC-Co coating, Ceramics International, 27, 2001, 669-674.
- [11] R. S. Lima, J. Karthikeyan, C. M. Kay, J. Lindemann and C. C. Brendt, Microstructural characteristics of cold-sprayed

- nanostructured WC-Co coatings, *Thin Solid Films*, 416, 2002, 129-135.
- [12] P. Bansal, N. P. Padture and A. Vasiliev, Improved interfacial mechanical properties of Al₂O₃-12wt%TiO₂ plasma-sprayed coatings derived from nanocrystalline powders, *Acta Materialia*, 51, 2003, 2959-2970.
- [13] Y. Zeng, S. W. Lee and C. X. Ding, Plasma spray coatings in different nanosize alumina, *Materials Letters*, 57, 2002, 495-501.
- [14] H. Kim, C. Lee and S. Hwang, Superhard nano WC-12%Co coating by cold spray deposition, *Materials Science and Engineering A* 391, 2005, 243-248.
- [15] X. Qi, N. Eigen, E. Aust, F. Gartner, T. Klassen and R. Bormann, Two-body abrasive wear of nano- and microcrystalline TiC-Ni-based thermal spray coatings, *Surface and Coatings Technology*, 200, 2006, 5037-5047,
- [16] Y. Zhu, K. Yukimura, C. Ding and P. Zhang, Tribological properties of nanostructured and conventional WC-Co coatings deposited by plasma spraying, *Thin Solid Films*, 388, 2001, 277-282.
- [17] G. Bolelli, B. Bonferroni, V. Cannillo, R. Gadow, A. Killinger, L. Lusvardi, J. Rauch and N. Steigler, Wear behavior of high velocity suspension flame sprayed (HVSFS) Al₂O₃ coatings produced using micron- and nano-sized powder suspensions, *Surface and Coatings Technology*, 2010, doi: 10.1016/j.surfcoat.2010.02.018
- [18] M. Roy, A. Pauschitz, R. Polak and F. Franek, Comparative evaluation of ambient temperature friction behaviour of thermal sprayed Cr₃C₂-25(Ni₂₀Cr) Coatings with conventional and nano-crystalline grains, *Tribology International*, 39, 2006, 29-38.

- [19] H. Chen, Y. Zhang and C. Diang, Tribological properties of nanostructured zirconia coatings deposited by plasma spraying, *Wear*, 253, 2002, 885-893.
- [20] S. Y. Park, M. C. Kim and C. G. Park, Mechanical properties and microstructure evolution of the nano WC-Co coatings fabricated by detonation gun spraying with post heat treatment, *Materials Science and Engineering, A* 449-451, 2007, 894-897.
- [21] Y. Wang, W. Tian and Y. Yang, Thermal shock behavior of nanostructured and conventional Al₂O₃/13 wt% TiO₂ coatings fabricated by plasma spraying, *Surface and Coatings Technology*, 201, 2007, 7746-7754.
- [22] R. S. Lima and B. R. Marple, Nanostructured YSZ thermal barrier coatings engineered to counteract sintering effects, *Materials Science and Engineering, A* 485, 2008, 182-193.
- [23] T. Rabizadeh, S. R. Allahkaram and A. Zarebidaki, An investigation on effects of heat treatment on corrosion properties of Ni-P electroless nano-coatings, *Materials and Design*, 2010, doi: 10.1016/j.matdes.2010.02.027
- [24] Q. Yu, C. Zhou, H. Zhang and F. Zhao, Thermal stability of nanostructured 13 wt% Al₂O₃-8 wt% Y₂O₃-ZrO₂ thermal barrier coatings, *Journal of the European Ceramic Society*, 30, 2010, 889-897.
- [25] J. H. Kim, K. H. Baik, B. G. Seong and S. Y. Hwang, Effects of post-spraying heat treatment on wear resistance of WC-Co nanocomposite coatings, *Materials Science and Engineering, A* 449-451, 2007, 876-879.
- [26] N. Wang, C. Zhou, S. Gong and H. Xu, Heat treatment of nanostructured thermal barrier coating, *Ceramics International*, 33, 2007, 1075-1081.
- [27] T. Y. Cho, J. H. Yoon, K. S. Kim, K. O. Song, Y. K. Joo, W. Fang, S. H. Zhang, S. J. Youn, H. G. Chun and S. Y. Hwang, A

- study on HVOF coatings of micron and nano WC-Co powders, *Surface and Coatings Technology*, 202, 2008, 5556-5559.
- [28] R. S. Lima and B. R. Marple, From APS to HVOF spraying of conventional and nanostructured titania feedstock powders; a study on the enhancement of the mechanical properties, *Surface and Coatings Technology*, 200, 2006, 3428-3437.
- [29] A. Ibrahim, R. S. Lima, C. C. Brendt and B. R. Marpl, Fatigue and mechanical properties of nanostructured and conventional titania (TiO₂) thermal spray coatings, *Surface and Coatings Technology* 201, 2007, 7589-7596.
- [30] T. Cui, J. Wang, R. Guan, L. Chen and G. Qiu, Microstructures and propertied of thermal barrier coatings plasma-sprayed by nanostructured zirconia, *Proceedings of Sino-Swedish Structural Materials Symposiun 2007*.
- [31] C. Liu, Z. Zhang, X. Jiang, M. Liu and Z. Zhu, Comparison of thermal shock behaviors between plasma-sprayed nanostructured and conventional zirconia thermal barrier coatings, *Trans. Nonferrous Met. Soc, China*, 19, 2009, 99-107.
- [32] P. Fogarassy, F. Gerday and A. Lodini, Agglomerated nanostructured particles disintegration during the plasma thermal spraying process, *Mechanics Research Communications*, 32, 2005, 221-239.
- [33] M. L. Lau, V. V. Gupta and E. J. Lavernia, Particle behavior of nanocrystalline 316-stainless steel during high velocity oxy-fuel thermal spray, *Nanostructured Materials*, 12, 1999, 319-322.
- [34] M. Gaona, R. S. Lima, B. R. Marple, Influence if particle temperature and velocity on the microstructure and mechanical behaviour of high velocity oxy-fuel (HVOF)-sprayed nanostructured titania coatings, *Journal of Materials Processing Technology*, 198, 2008, 426-434.

- [35] L. L. Shaw, D. Goberman, R. Ren, M. Gell, S. Jiang, Y. Wang, T. D. Xiao and P. T. Strutt, The dependency of microstructure and properties of nanostructured coatings on plasma spray conditions, *Surface and Coatings Technology*, 130, 2000, 1-8.
- [36] R. S. Lima, A. Kucuk and C. C. Brendt, Evaluation of microhardness and elastic modulus of thermally sprayed nanostructured zirconia coatings, *Surface and Coatings Technology*, 135, 2001, 166-172.
- [37] B. R. Marple, J. Voyer, J. F. Bisson and C. Moreau, Thermal spraying of nanostructured cermet coatings, *Journal of Materials Processing Technology* 117, 2001, 418-423.
- [38] www.castolin.com/wCastolin_com/products/welding/endotec.php
- [39] P. Miao, G.R. Odette, J. Gould, J. Bernath, R. Miller, M. Alinger, C. Zanis, The microstructure and strength properties of MA957 nanostructured ferritic alloy joints produced by friction stir and electro-spark deposition welding, *Journal of Nuclear Materials* 367–370 (2007) 1197–1202.
- [40] B.S. Yilbas, M. Sunar, Z. Gasem, B.J. Abdul Aleem, S.Zainaulabdeen, Study into mechanical properties of TiN coating on Ti-6Al-4V alloy through three-point bending tests", *Industrial Tribology*, 57, 2005, 193-196.
- [41] Z. Y. Taha-al, M. S. J. Hashmi, B. S. Yilbas, Effect of WC on the residual stress in the laser treated HVOF coating, *J. Material Processing Technology*, 209, 2009, 3172-3181.

Publications by the Author

- A. Al-Askandarani, M.S.J. Hashmi, B.S. Yilbas, Coating produced by deposition of nanoparticles blended wires, conference on Advances in Materials and Processing Technologies, AMPT09, Kuala Lumpur, Malaysia, November 26-29, 2009.
- A. Al-Askandarani, M.S.J. Hashmi, B.S. Yilbas, Arc spraying of nano-structured wire on carbon steel: examination of coating microstructures , conference on Advances in Materials Processing Technology, AMPT10, Paris, France October 24-27, 2010.